Environmental Pollution 330 (2023) 121726

Contents lists available at ScienceDirect

Environmental Pollution

journal homepage: www.elsevier.com/locate/envpol

The impacts of ambient ozone pollution on China's wheat yield and forest production from 2010 to 2021 ☆

Yutong Wang [a], Youchao Wang [a], Zhaozhong Feng [c], Xiangyang Yuan [c], Yu Zhao [a,b,*]

[a] State Key Laboratory of Pollution Control and Resource Reuse, and School of Environment, Nanjing University, 163 Xianlin Rd., Nanjing, Jiangsu, 210023, China
[b] Jiangsu Collaborative Innovation Center of Atmospheric Environment and Equipment Technology (CICAEET), Nanjing University of Information Science and Technology, Jiangsu, 210044, China
[c] Key Laboratory of Ecosystem Carbon Source and Sink, China Meteorological Administration (ECSS-CMA), Key Laboratory of Agrometeorology of Jiangsu Province, School of Applied Meteorology, Nanjing University of Information Science & Technology, Nanjing, China

ARTICLE INFO

Keywords:
Ozone damage
Simplified metric
Spatial distribution
Interannual trend
Main driver

ABSTRACT

Near-surface ozone causes damages on both crop and forest but their long-term spatiotemporal changes in China have been insufficiently explored, preventing comprehensive policy making with food security and climate targets. Moreover, limitation exists in the current metrics for long-term regional ozone risk assessment, AOT40 (the accumulated hourly ozone over a threshold of 40 ppbv) and POD_Y (phytotoxic ozone dose over a threshold of Y nmol ozone m^{-2} PLA s^{-1}), with ignorance of meteorological influence for the former and complicated data collection and calculation procedures for the latter. Here, we developed a new metric for ozone-induced risk on winter wheat, O3MET, which can be easily derived based on ozone concentrations and meteorological variables, and is suitable for long-term assessment of ozone-induced wheat loss at the regional scale. Combining with existing metric for forest (O3RH), we comprehensively quantified the ozone damages on winter wheat yield and forest gross primary production (GPP) for mainland China during 2010–2021, the period with fast growth of ozone level across the country. The annual average losses of wheat yield and forest GPP were estimated at 26.5 Mt and 552.6 TgC, accounting for 17% and 4% of the total yield and GPP without ozone impact, respectively. Heavy dual ozone-induced damages on both wheat and forest were presented in East and South China. The ozone-induced wheat yield loss and forest GPP loss were estimated to increase at a rate of 1.8 Mt/yr and 13.9 TgC/yr for the entire country, respectively, driven mainly by the enhanced ambient ozone level within the research period. Besides ecological impact, the ozone pollution in the developed eastern China resulted in serious health burden as well, thus effective actions on ozone pollution alleviation in the region is crucial for reducing its ecological and health risks simultaneously.

1. Introduction

Near-surface ozone is produced through photochemical reactions of nitrogen oxides (NO_X) and volatile organic compounds (VOCs), under the condition with relatively high temperature and low humidity. It impairs plant photosynthesis and accelerates plant senescence, ultimately leading to lower plant protein and yields (Feng et al., 2008, 2011; Broberg et al., 2015). Given its complex nonlinear response to precursors, China's ozone pollution level has kept increasing and reached the peak by 2019, even with stringent emission control actions since 2013 (Li et al., 2020). To stress the air quality and climate issue simultaneously, China is conducting a series of polices on energy structure adjustment and industrial pollutant abatement, under the carbon peaking and carbon neutrality strategy. Even with a declining trend, the future ozone level is predicted to be still larger than the World Health Organization standards (100 μg/m^3) for a long period (Shi et al., 2021), leading to a continuous damage on crops and forests.

As the third most important crop with a global production of 775 million tons in 2021 (FAO, 2022), wheat is a plant susceptible to ozone exposure, and exaggerating ozone pollution was estimated to undermine the efforts to increase wheat yields over the world (Feng et al., 2022; Mills et al., 2018; Tai and Martin, 2017). China is the largest wheat

☆ This paper has been recommended for acceptance by Alessandra De Marco.

* Corresponding author. State Key Laboratory of Pollution Control and Resource Reuse and School of the Environment, Nanjing University, 163 Xianlin Ave., Nanjing, Jiangsu, 210023, China.
E-mail address: yuzhao@nju.edu.cn (Y. Zhao).

https://doi.org/10.1016/j.envpol.2023.121726
Received 1 March 2023; Received in revised form 17 April 2023; Accepted 25 April 2023
Available online 29 April 2023
0269-7491/

producing nation, accounting for 17.5% of global wheat yield, and the proportion of winter wheat reached 94% of total production (Feng et al., 2019a,b). Precise quantification of the impact of increasing ozone pollution on yield loss of winter wheat provides important scientific basis to stress the national food security in China. Besides, China has been implementing one of the most ambitious afforestation programs in the world to elevate the ecological restoration and carbon sink of terrestrial ecosystems (Zhang et al., 2017). However, ozone pollution can weaken the gross primary productivity (GPP) of vegetation, and further reduce the uptake of carbon dioxide (CO_2) by plants. It is identified as one of the most important factors affecting carbon sink in terrestrial ecosystems (Yue et al., 2017). Most of existing studies evaluated single ozone-induced impact on vegetation (crop yield or forest productivity), but rarely explored the similarity and difference in spatial and temporal distribution between the two. A comprehensive analysis on both crop and forest damages attributable to ozone exposure, as well as their main drivers, will substantially improve the understanding of the diversity and complexity of ecological impact of ozone pollution, and help policy design to reduce ozone pollution more reasonably and efficiently.

Ozone damaging metrics can be classified into two categories. One is the ozone exposure metric represented by AOT40, which is defined as the cumulative value of hourly ozone concentration exceeding 40 ppbv during plant growing season. The other is the ozone flux metric represented by POD_Y (phytotoxic ozone dose over a threshold of Y nmol ozone m^{-2} PLA s^{-1}), which takes into account not only the ozone concentration and exposure time, but also the influence of biological and environmental conditions on leaf stomatal conductance. As it reflects the actual stomatal ozone uptake flux of plants, POD_Y is superior to AOT40 in assessing the adverse effects of ozone on plants. Feng et al. (2019a,b) assessed the ozone-induced yield loss of winter wheat in China from 2015 to 2016 using AOT40 and POD_{12}, respectively, and found smaller yield loss calculated with POD_{12} than AOT40 and clear variability in spatial distribution between the two. However, the estimation of POD_Y requires hourly ozone concentrations and a series of factors representing environmental stresses and phenology. Station level POD_Y can be relatively easy to access, but the complexity of the calculation process for each factor and the difficulty of obtaining hourly ozone concentrations and meteorological data (such as photosynthetic photon flux density, soil water potential) with full spatial and temporary coverage make it difficult to assess the ozone risk over large areas and long time series. The ozone exposure metric AOT40 has been more commonly applied in quantifying the effect of ozone pollution on crop yield and forest productivity at the regional or globe scales (Feng et al., 2022; Ren et al., 2020; Feng et al., 2019a,b; Zhao et al., 2018; Li et al., 2020; Tai and Martin, 2017). Such application could easily exaggerate the role of ambient ozone concentration change on driving the spatial and temporal variation of ozone-induced damage, as the influences of meteorological factor on vegetation were not considered. The limitation would prevent correct understanding of the causes of ozone-related risks and reasonable policy making of pollution alleviation. For forest ecosystem, Gong et al. (2021) established a new metric O3RH, which incorporates ozone levels and meteorological factors and can be simply derived using daily ozone concentrations and relative humidity, to assess the long-term ozone risk assessment on vegetation GPP at the regional scale. While a new metric with simplified procedure and easily accessible input data is still missing in the assessment of long-term trends and spatial patterns of ozone impacts on crop production.

To date, very few studies comprehensively investigated long-term ozone impacts on crop production and forest GPP in China with integrated consideration of meteorological factors and ozone concentrations. This study, therefore, combined a high-resolution ozone concentration dataset obtained through a modified machine learning technique and a generalized additive model (GAM) to develop a new metric (O3MET) for assessing the ozone-induced risk on winter wheat. We then applied O3MET to estimate the long-term spatiotemporal patterns of ozone impact on wheat yield, as well as the main drivers of changing wheat and forest loss. We also applied O3RH developed by Gong et al. (2021) to estimate the long-term variability of ozone-induced forest GPP loss and its main drivers. We further assess the similarity and difference in spatial and temporal distributions between the two categories of ozone-induced risks on vegetation, for better policy making of ozone pollution abatement.

2. Methods and materials

2.1. Simplified metrics considering ozone and meteorology factors for calculation of wheat yield and forest GPP loss

To easily and effectively quantify the long-term winter wheat yield loss from ozone pollution at the regional scale, we developed a simplified metric (O3MET) that includes the influences of both near-surface ozone level and meteorological factors, following the steps described below. First, based on available POD_{12} and AOT40 estimations at 273 stations in China in 2015 and 2016 (Feng et al., 2019a,b), we defined an index g_{met} as POD_{12}/AOT40, which represents the effect of meteorological factors on the magnitude of ozone uptake by wheat. The equations of POD_{12} and AOT40 calculation are described in Text Section 1 in the Supplement.

To predict the spatiotemporal pattern of g_{met} across the country, we then derived a generalized additive model (GAM), which applied smoothing function (s (3)) to describe the nonlinear relationship between g_{met} and key meteorology factors affecting the calculation of stomatal conductance (reflected by f_{light}, f_{temp}, f_{swp}, and f_{vpd}, in Eq. S4 in the Supplement). Those include the total precipitation (TP), 2 m-tempreture (T2M) and surface downwelling shortwave radiation (RSDS):

$$g_{met} = s(TP) + s(T2M) + s(RSDS) \tag{1}$$

Finally, the simplified metric O3MET can be determined as:

$$O3MET = \max((O_3\text{-}TH) \times \max(g_{met},0),0) \tag{2}$$

where O_3 represents growing season-averaged maximum daily average 8-h (MDA8) ozone concentration (ppbv), and TH is the threshold of MDA8 ozone concentration for wheat damage (ppbv). Attributed to the detoxification mechanism of vegetation for harmful substances, ozone-induced damage is expected to only occur when MDA8 ozone concentration is larger than TH. We calculated the Pearson correlation coefficients between POD_{12} and O3MET estimated with different optional TH levels, and 30 ppbv was finally chosen, with the strongest correlation ($R = 0.73$) found between O3MET and POD_{12} (Fig. S1 in the Supplement).

O3RH is a simplified ozone damaging metric for vegetation GPP developed by Gong et al. (2021) that can be applied to deciduous broadleaf forest, evergreen coniferous forest, and evergreen broadleaf forest.

$$O3RH = f(O_3) \times f(RH) \tag{3}$$

$$f(O_3) = \max(0, O_3\text{-}20) \tag{4}$$

$$f(RH) = \max(0, \min(RH\text{-}40\%, 40)) \tag{5}$$

where O_3 is the growing season-averaged MDA8 ozone concentrations (ppbv) and RH is the growing season-averaged relative humidity (%).

Due to the large extent of wheat and forest planting from cold temperate to tropical climate in China, we defined the duration of vegetation growing season according to their geographic distribution. For wheat, the growing season was defined from 45 days before flowering to 30 days after flowering (Feng et al., 2019a,b). We obtained the gridded flowering data of wheat through Kriging interpolation based on station observations. For forest, the growing season was defined by a simple latitude model (UNECE, 2017). Fig. S2 in the Supplement illustrates the spatial distribution of the day of year (DOY) for the start and end of growing season of wheat and forest.

We obtained relative yield loss (RYL) for winter wheat at 273 stations using POD_{12} estimations and flux-based response function reported in Feng et al. (2019a,b). We further established the relationship between O3MET and RYL of winter wheat (Eq. (6)) by performing a linear regression to the estimated RYL and O3MET at 273 stations. The square of correlation coefficient (R^2) reached 0.53 (see detailed analysis evaluation in Section 3.1). Wheat yield loss (WYL) was then calculated based on wheat yield (WY) and relative yield loss (RYL) with Eq. (7).

$$RYL = 0.026 \times O3MET + 0.016 \quad (6)$$

$$WYL = WY/(1\text{-RYL}) \times RYL \quad (7)$$

Similarly, relative loss for forest GPP (RPL) was calculated with Eq. (8), which represents the multi-year average of the relationship between O3RH and RPL developed by Gong et al. (2021). The forest GPP loss (GPL) was calculated based on forest GPP and RPL using Eq. (9).

$$RPL = 0.0065 \times O3RH - 0.0092 \quad (8)$$

$$GPL = GPP/(1\text{-}RPL) \times RPL \quad (9)$$

2.2. Data sources of ozone-wheat risk measurements, MDA8 ozone concentrations and meteorological and ecological information

Estimations for POD_{12} and AOT40 at 273 stations in China were collected for 2015 and 2016 from Feng et al. (2019a,b). MDA8 ozone concentrations were estimated with an optimized machine learning model (Xgboost) at a horizontal resolution of 0.1° × 0.1°, as described in our previous work (Wang et al. under review in Nature Geoscience). Xgboost model developed the comprehensive relationship between MDA8 ozone concentrations and both meteorological and chemical variables year by year, and satisfying model performances were achieved for all years for the country (Fig. S3 in the Supplement). Meteorological parameters used for calculating ozone damaging risk were obtained from the fifth generation European Centre for Medium-Range Weather Forecasts (ECMWF) climate reanalysis (ERA5) with a horizontal resolution at 0.1° × 0.1°. The annual wheat yield data from 2010 to 2021 were obtained from the China Statistical Yearbook by province and then were gridded with a horizontal resolution at 10km × 10 km, according to the geographic distribution of wheat yield (Monfreda et al., 2008). The gridded GPP data from 2010 to 2021 were extracted from Moderate-Resolution Imaging Spectroradiometer (MODIS) MOD17A2H product at a temporal resolution of 8 days and a horizontal resolution of 500 m (https://search.earthdata.nasa.gov/search?q=MOD17A2H, last access: December 2022). We divided the original data of the product by 8 to obtain the daily average GPP for the period. We further obtained gridded forest GPP data based on the forest biomass distribution map (https://geodata.cn). We used bilinear interpolation to resampled the meteorological data, wheat yield data and forest GPP data to the 0.1° × 0.1°grid, consistent with the grid of MDA8 ozone concentrations. As a summary, Fig. S4 in the Supplement briefly shows the workflow of this work, including data processing, model construction and prediction. In particular, the model evaluation of wheat yield loss will be presented in details in Section 3.1.

3. Results and discussions

3.1. Evaluation and application of O3MET

Fig. S5a in the Supplement shows the performance of GAM which connected g_{met} and meteorology factors. The correlation between prediction and observation ($R = 0.55$, $p < 0.05$) indicates the model is capable of capturing the spatiotemporal variation of g_{met}. As a reference, the R commonly ranged between 0.39 and 0.84 in previous studies that applied statistical models to explore the effect of meteorological factors on plant growth (Dai et al., 2019; Mulder et al., 2017; Wang et al., 2015). The model residuals are normally distributed (Fig. S5b), implying the model contained all the important influencing factors. The variance inflation factors (VIF, $1/(1\text{-}R^2)$, with R^2 obtained from the regression of each explanatory variable against all other explanatory variables present in the model) for all meteorological factors are smaller than the threshold of 5 (1.17, 1.68 and 1.48 for TP, T2M, and RSDS respectively), indicating that there is no multicollinearity for the model (Huang et al., 2020).

Fig. S6 in the Supplement shows the partial response of meteorological factors to g_{met}, and complex non-linear relationships between individual factors and g_{met} are found. Basically g_{met} rises with increasing TP even some fluctuations exist, as the elevated TP makes stomata open. Within the temperature range containing a large number of sampling points (285–290 K), g_{met} increases with growing temperature because leaves need to resist heat through enhanced transpiration by stomata. However, when the temperature is higher than 287 K, wheat reduces stomatal conductance to prevent excessive water loss from leaf, resulting in a declining g_{met}. With growing light, g_{met} increases first and then decreases. At relatively low level, the increasing solar radiation can promote photosynthesis in plants, resulting in expanded stomata to absorb more CO_2. When solar radiation reaches a certain threshold (1.1e+07 J/m^2), further enhancement causes damage to the surface of plant leaves and thereby decreases stomatal conductance. As shown in Fig. 1, the spatial distribution of 2015–2016 averaged g_{met} predicted by GAM was consistent with the site-level result combining POD_{12} and AOT40. The site-level g_{met} was calculated to range from 0.01 to 1 and larger values occurred in Jiangsu and Anhui with relatively high temperature, radiation and precipitation.

As described in Section 2.1, O3MET was obtained by combining g_{met} and ozone levels, and then applied to estimate RYL in this work (Eqs. (2) and (6)). Table S1 in the Supplement summarize and compare different metrics and ozone-yield response functions for agricultural crops reported by a variety of studies. The square of correlation coefficient (R^2) of our model (0.53) is within the range of others (0.20–0.96). Given much more data points (and thereby scattered ones) of our model than those of others, we believe application of O3MET as a metric to evalue RYL is reasonable. To further prove the reliability of O3MET, we calculated the correlation coefficient and mean normalized bias between O3MET-based RYL (this work) and POD_{12}-based RYL (Feng et al., 2019), as shown in Fig. S7 in the Supplement. The correlation coefficients for both 2015 and 2016 were greater than 0.75, and limited the mean

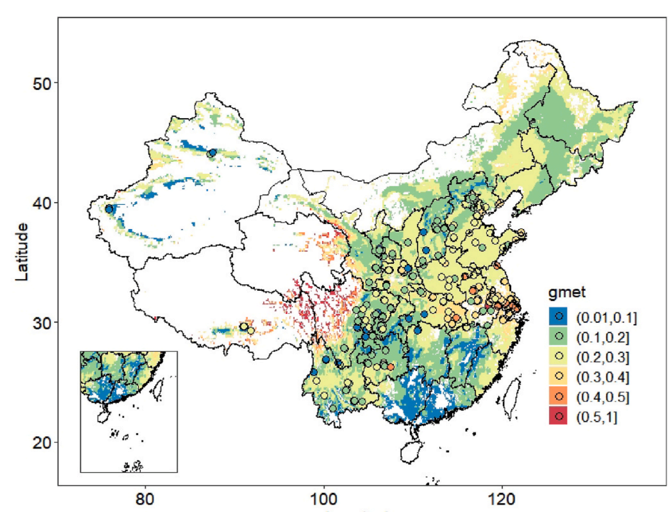

Fig. 1. The 2015–2016 averaged g_{met} predicted from GAM (background) and that estimated from POD_{12} and AOT40 at 273 stations (circle).

normalized biases were found for the main wheat producing provinces, indcluding Hebei (−0.8%~9%), Henan (16%~27%), Shandong (5%~19%) and Anhui (−28%~22%). The comparion thus again justifies the application of O3MET.

3.2. Spatial distribution of ozone damaging metrics

Combining meteorological data and MDA8 ozone concentrations, we calculated O3MET and O3RH during the growing season of wheat and forest, respectively, for 2010–2021. Fig. 2a shows the spatial distribution of O3MET on average between 2010 and 2021, with considerable variability for regions and provinces (see the region and province definitions in Fig. S8 in the Supplement). Hotspots of O3MET were located mainly in Northwest and East regions, especially in Qinghai (6.7 ppbv), Tibet (6.5 ppbv), Shandong (6.4 ppbv) and Shanghai (6.2 ppbv). The areas with relatively low O3MET were located in South region, especially Guangdong (1.0 ppbv), Guangxi (1.0 ppbv), Chongqing (1.6 ppbv) and Hunan (1.8 ppbv). The spatial distributions of O3MET and MDA8 ozone concentration were not completely consistent with each other, as O3MET was also influenced by stomatal conductance indicated by g_{met}. For example, even though the MDA8 ozone concentrations in Northwest region (e.g. Qinghai and Tibet) were much lower than in East region (e.g. Shandong and Shanghai, Fig. S9a in the Supplement), relatively high O3MET was still found for the former while the values were relatively low for some provinces with high MDA8 ozone concentrations in the latter (e.g. 5.0 ppbv for Hebei, Fig. 2a). The stronger solar radiation in Northwest region promoted stomata opening, and consequently enhanced g_{met} (Fig. S9b) and ozone damage on wheat.

The high O3RH existed mainly in East and South regions (Fig. 2b), especially in Jiangsu (11.0 ppbv), Shandong (9.9 ppbv), Anhui (9.8 ppbv) and Hubei (9.4 ppbv) with both high MDA8 ozone concentrations and RH (Figs. S9c and d). Most of the provinces with low O3RH were located in Northwest and Northeast regions, especially Inner Mongolia, Ningxia, Heilongjiang and Xinjiang with the values smaller than 6.0 ppbv. Similar with O3MET, although MDA8 ozone concentrations in some northern provinces (e.g., Hebei) were higher than southern ones (Fig. S9c), smaller O3RH were estimated for the former, attributed to the lower RH (Fig. S9d).

3.3. Ozone-induced wheat yield loss and forest GPP loss across China

3.3.1. Spatial distribution

We calculated the ozone-induced wheat yield loss combining the annual wheat yield and O3MET estimated in Section 3.2. During 2010–2021, the annual average of winter wheat yield loss was estimated at 26.5 Mt in mainland China, accounting for 17.3% of the gross wheat yield without ozone impact. Fig. 3a and Fig. S10b in the Supplement shows the spatial distributions of the annual ozone-induced wheat yield loss and gross wheat yield without ozone impact averaged between 2010 and 2021, respectively. The spatial pattern of O3MET (Fig. 2a) was close to that of gross wheat yield (Fig. S10a), i.e., relatively large yield is found in East and Northwest regions and small in Northeast and South regions. The consistency of spatial distribution between O3MET and wheat yield thus resulted in severe ozone damage in the main wheat producing areas. The annual average yield losses were estimated at 24.3, 1.2, 0.3, and 0.7 Mt for East, Northwest, Northeast and South regions, accounting for 92.0%, 4.5%, 1.1%, and 2.4% of the national total loss, respectively (Table S2 in the Supplement). East region has experienced the most serious ozone-induced damage on wheat yield, with the largest loss found in Henan, Shandong, Anhui and Hebei provinces at 7.4, 5.1, 4.2, and 2.9 Mt averaged during 2010–2021, respectively (Fig. 3a and Table S2).

The forest GPP loss was calculated by combining O3RH and forest GPP data. National forest GPP loss was 552.6 TgC on average during 2010–2021, accounting for 3.9% of gross forest GPP without ozone impact. Fig. 3b and Fig. S10b show the spatial distributions of the annual ozone-induced forest GPP loss and gross forest GPP without ozone impact averaged between 2010 and 2021. Areas with serious forest GPP losses were located in the southeastern coastal areas including Zhejiang, Fujian, Guangdong and Guangxi provinces, with the annual average GPP loss estimated at 16.7, 22.3, 32.1, and 33.3 TgC, respectively (Fig. 3b and Table S2). Both high forest GPP (Fig. S10b) and O3RH (Fig. 2b) were found in those areas. Even with a dense forest distribution (Fig. S10b), the forest GPP loss in certain northeastern provinces (e.g., Inner Mongolia) was smaller than some regions with sparse forest cover (e.g. East region) due to the smaller O3RH for the former. The annual average GPP losses were estimated at 288.4, 125.1, 40.6 and 98.5 TgC for South, East, Northwest and Northeast regions, accounting for 52.2%, 22.6%, 7.3% and 17.8% of the national total loss, respectively (Table S2).

Incorporating wheat yield loss and forest GPP losses, we assessed the spatial pattern of ozone-induced damage on vegetation comprehensively, as shown in Fig. 3c. Clear variability existed in the distribution of two categories of ozone-induced damage across the country. Wheat yield loss was more prevalent in northern areas, while forest GPP loss was more prevalent in southern ones. In East and South regions, especially in Hebei, Shandong, Hubei and Sichuan provinces, dual ozone-induced damages on both wheat and forest were presented. Besides, as shown in Fig. S2, the ozone damage on wheat yield started in

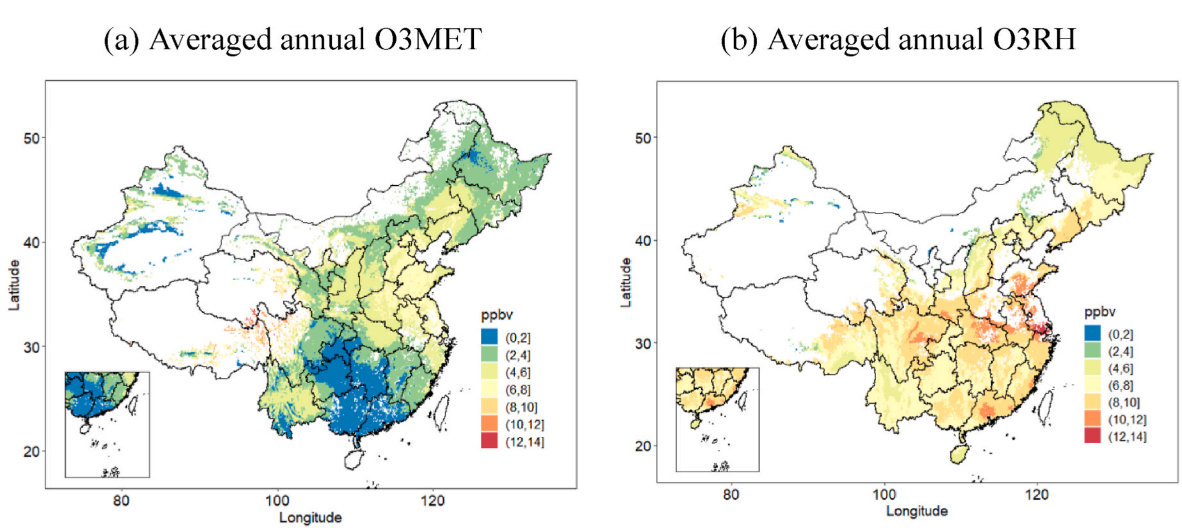

Fig. 2. Spatial distribution of ozone damaging metrics averaged between 2010 and 2021: (a) O3MET; (b) O3RH. The horizontal resolution is 0.1° × 0.1°. White represents areas without winter wheat or forest cover.

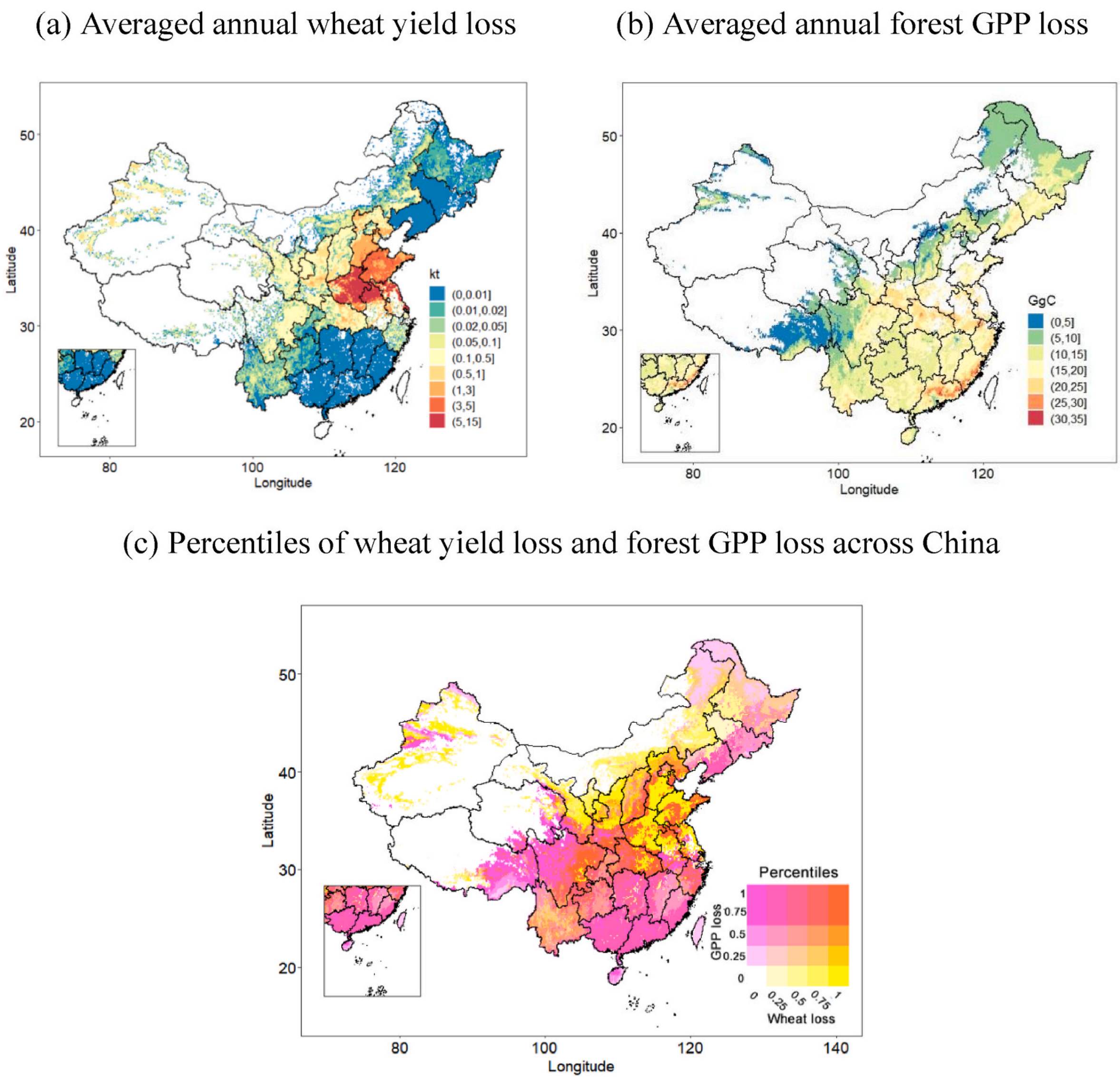

Fig. 3. Spatial distributions of the multiple-year averages of annual winter wheat yield loss (a), forest GPP loss (b) and the percentiles of wheat yield loss and forest GPP loss across China (c). Yellow represents more severe wheat yield loss, pink represents more severe forest GPP loss, and orange represents the severe dual ozone damages. (For interpretation of the references to colour in this figure legend, the reader is referred to the Web version of this article.)

February–March, earlier than that on forest GPP (March–April). The damage ended in May–June for wheat yield and in October–December for forest GPP. For the above-mentioned regions with abundant dual ozone-induced ecological impacts (part of South and East regions), typically, the growing season last from mid-February to late May for wheat and from late March to early December for forest. Forests were subjected to longer ozone stress than wheat, with March–May being the period when dual ozone-induced damages occurred. As the period was commonly of high ambient ozone levels within the whole year for those areas, implementation of effective measures on ozone pollution alleviation can result in great benefits on both ecological metrics.

3.3.2. Interannual trend

We investigated the interannual variation of ozone-induced damages on wheat yield and forest GPP during 2010–2021 for entire China and key regions. As shown in Fig. 4a, the nationwide ozone-induced wheat yield loss increased significantly from 17.1 Mt in 2010 to 36.1 Mt in 2018, followed by a decline to 29.9 Mt in 2021. The annual growth rate of wheat yield loss (10%/yr or 1.8 Mt/yr) was much higher than that of wheat yield without ozone impact (3%/yr) during 2010–2021, implying the overall growing ozone stress on the wheat. The declining yield loss after 2018 resulted possibly from the restrained ozone level for the most recent years.

To identify the main driver of increased interannual ozone stress, we compared the correlation coefficient between MDA8 ozone and wheat yield loss and that between g_{met} and wheat yield loss, and then defined the variable with larger correlation coefficient as the main driver. For the entire country, MDA8 ozone shows a much stronger correlation with wheat yield loss ($R = 0.85$) than g_{met} ($R = 0.05$), thus the significant ozone growth during the wheat growing season at a rate of 2%/yr was recognized as the major reason for the increasing wheat yield loss. Similarly, the increasing wheat yield losses in the East, Northwest, and Northeast regions were also estimated to be driven by the elevated MDA8 ozone concentrations (Figs. S11a–c in the Supplement). In South region, however, the wheat yield loss declined slightly attributed partly to the reduced wheat production (Fig. S11d). The annual declining rate of yield loss (0.5%/yr) was smaller than that of total yield (4%/yr), which was more affected by the growth of g_{met} ($R = 0.71$) rather than MDA8 ozone ($R = 0.20$). Fig. S12a in the Supplement shows the relationship among MDA8 ozone concentration, g_{met} and O3MET. As MDA8

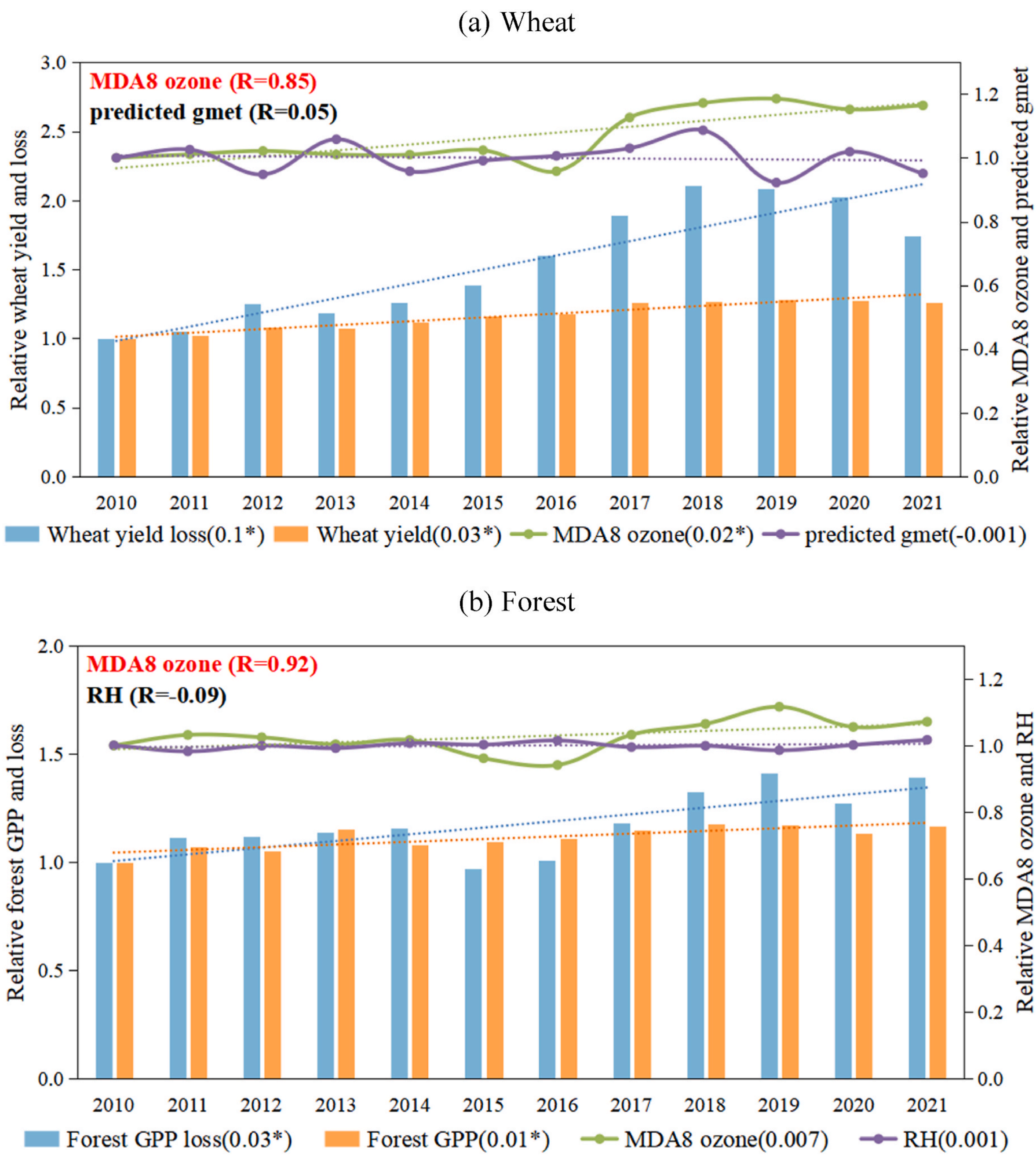

Fig. 4. Interannual trends of ozone-induced damage on vegetation and their drivers during 2010–2021: (a) Ozone-induced wheat yield loss, wheat yield without ozone impact, MDA8 ozone and g_{met} predicted from Eq. (1); (b) Ozone-induced forest GPP loss, forest GPP without ozone impact, MDA8 ozone and RH. The values are normalized to 2010 level and linear regression model of the time series are performed. Interannual rates (unit:/yr) of those variables are in parentheses (* represents $p < 0.05$). The correlation coefficients (R) between ozone-induced damage and drivers are provided in the upper left corner of each panel. The driver with larger R is marked in red. (For interpretation of the references to colour in this figure legend, the reader is referred to the Web version of this article.)

ozone shifts from low to high concentration, O3MET is increasingly sensitive to the variation in g_{met}, indicating the importance of stomatal opening on ozone absorption under high ozone exposure. Similarly, compared to small g_{met} condition with limited stomata openness, O3MET is more sensitive to the variation in MDA8 ozone with elevated g_{met} and stomata openness. In Northwest, Northeast and East regions where g_{met} was relatively large (greater than 0.2 for regional average), the ozone damage was more susceptible to the MDA8 ozone concentration. In South regions where g_{met} was smaller (<0.2), ozone uptake by wheat was more limited, thus the ozone-induced damage was more sensitive to the magnitude of g_{met}.

The ozone-induced forest GPP loss has basically kept growing for the entire country (3%/yr or 13.9 TgC/yr, Fig. 4b) and most regions (East, Northwest, and South regions, Fig. S13). Similar to wheat, the annual growth rates of GPP loss were larger than those of forest GPP without ozone impact for the entire country and most regions, implying the enhanced ozone stress on forest. The interannual trends of ozone-induced GPP loss were dominated by MDA8 ozone for all regions. Although O3RH is detected to be sensitive to the variation in RH at relatively high MDA8 ozone level (Fig. S12b), the growing forest GPP loss had little association with RH as the interannual variation in RH was very limited for all the regions (Fig. S13).

We compared our estimates in RYL and RPL during 2010–2021 with other studies in Fig. S14 in the Supplement. For ozone-induced wheat yield loss, our O3MET-based estimates are higher than the POD_{12}-based estimates and are smaller than AOT40-based estimates (Fig. S14a). The differences resulted mainly from the different consideration of meteorological limitations on ozone uptake in the indicators. Application of AOT40 resulted in a relatively high RYL because it ignores meteorological limitations on ozone uptake. The different calculation procedures between g_{met} in O3MET and stomatal conductance in POD_{12} caused O3MET-based estimates in RYL higher than that POD_{12}-based ones. For ozone-induced forest GPP loss, O3RH-based estimates in our study are smaller than AOT40-based ones and even smaller than those based on land carbon model (YIBS in Yue et al. (2017)), attributed mainly to the applications of different model mechanisms (Fig. S14b).

3.4. Policy implications and uncertainties

This study estimated the long-term impacts of ozone pollution on winter wheat yield and forest GPP for China, and clear difference was found between regions attributed to the diverse ozone levels, meteorological and phenological conditions. In this section, the ecological impacts of ozone pollution at the provincial level are further linked with its human health burden to help policy making of ozone pollution alleviation in a more comprehensive perspective. Besides ecological metrics RYL and WYL for wheat yield loss and RPL and GPL for forest GPP loss (Eqs. (6)–(9)), we also calculated an additional metrics PWCP (Population-weighted concentrations combined with Population) for each province to represent the ozone exposure on human health. The method of calculating PWCP can be found in Text Section 2 in the Supplement.

Fig. 5 shows the ecological metrics (RYL, WYL, RPL and GPL) and human health metrics (PWCP) for each province. According to 50th percentiles of relative loss and total damage, provinces are divided into four types. Provinces of Type I are of both high ozone-induced relative risk (i.e. RYL or RPL) and large damage (i.e. WYL or GPL) on vegetation, for example, Henan and Shandong for wheat (Fig. 5a), and Sichuan and Guangxi for forest (Fig. 5b). In those areas, ozone pollution alleviation is in urgent need to reduce its ecological damage. Although the relative risk might not high in some Type-II provinces, the ozone-induced damages were still large because of the relatively large amount of wheat and forest growing there, such as Hubei and Xinjiang for wheat, and Yunnan and Heilongjiang for forest. Further exacerbation of ozone pollution would elevate the vegetation loss and thus needs to be prevented in those provinces. For Type-III provinces, the total ozone-induced damages were modest even with a high relative risk, as they did not grow abundant crops or forest. Those include Qinghai and Tibet provinces for wheat, and Shandong and Jiangsu for forest. When possible, the vegetation that is not sensitive to ozone pollution should be recommended in those areas.

We further analyze the joint impacts of ozone pollution on ecology and health burden. Judged by the wheat, relatively high PWCP was found in areas with severe WYL (Types I and II), such as Henan, Shandong, Anhui, Hebei and Jiangsu (Fig. 5a). In contrast, for forest, high PWCP occurred more frequently in areas with smaller GPL (Types III and IV), and the association between ozone-induced ecological and health effects is weak (Fig. 5b). Most of the provinces with both large ozone-induced wheat yield loss and health burden are located in the East region, with developed industrial economy and high ambient ozone level. As described in Section 3.2.2, significant enhancement in MDA8 ozone concentration for the past decade drove the growth in WYL in the region, while it greatly changed the human exposure as well (Xiao et al., 2022). Effective and efficient actions on emission controls for the ozone precursors is crucial for reducing ozone-induced ecological and health damages in relatively developed and polluted regions in China.

Limitations exist in current study. There were not enough estimations of POD_{12} and AOT40, which were only conducted in the main wheat producing areas in 2015–2016. Insufficient metrics estimated using observations prevented a full evaluation on spatiotemporal distributions of O3MET and O3RH, as well as their interannual variations, from our estimation. For ozone risk assessment on crops, moreover, we considered only one crop, winter wheat, but ignored other crops that are subject to ozone stress, attributed also to the lack of estimations of ozone flux metrics for them. Future work is recommended to collect more POD_Y and to develop simplified metrics and dose-response relationships for different crop types, and more comprehensive understanding on ozone-induced ecological damage can be expected.

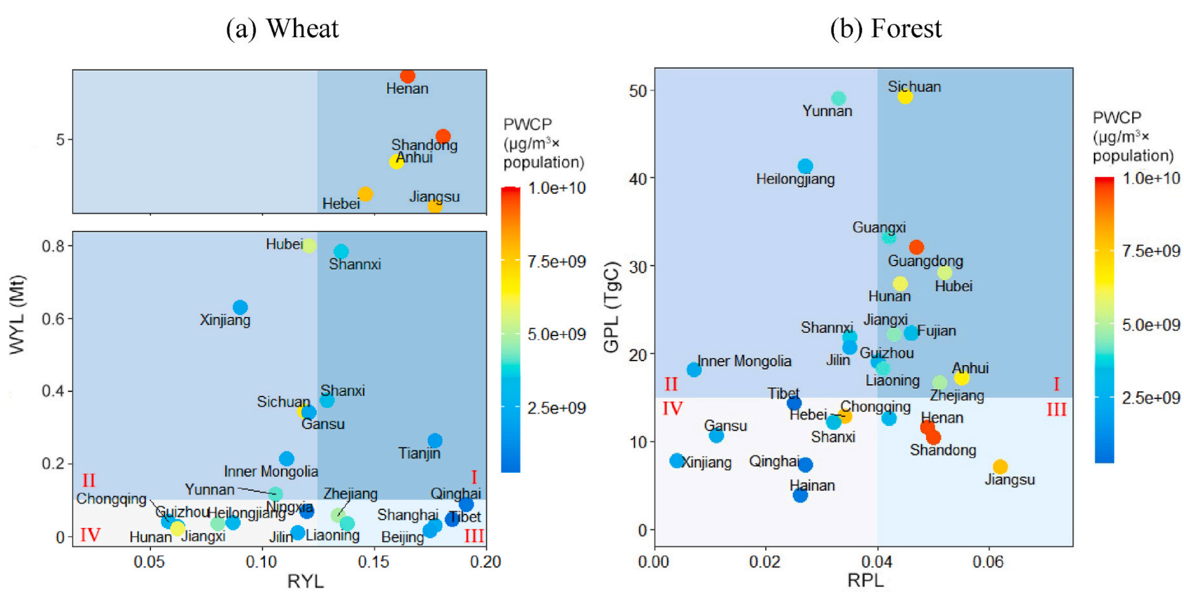

Fig. 5. Classification of provinces based on ozone-induced ecological and heath impacts. (a) Relative wheat yield loss (RYL), wheat yield loss (WYL) and ozone exposure on human health (PWCP) by province; (b) Relative forest GPP loss (RPL), forest GPP loss (WPL) and ozone exposure on human health (PWCP) by province. Note: Type I represents the combination of both RYL (RPL) and WYL (GPL) greater than the 50th percentile; Type II represents the combination of RYL (RPL) less than the 50th percentile and WYL (GPL) greater than the 50th percentile; Type III represents the combination of RYL (RPL) greater than the 50th percentile and WYL (GPL) smaller than the 50th percentile; and Type IV represents the combination of both RYL (RPL) and WYL (GPL) smaller than the 50th percentile. Provinces with WYL less than 0.01 Mt or GPL less than 1 TgC were excluded.

4. Conclusions

By combining a GAM model and a high-resolution ozone concentration dataset from machine learning, we develop a new metric (O3MET) to evaluate the long-term ozone-induced risk on winter wheat at the regional scale. We then applied O3MET and O3RH to explore the spatiotemporal pattern of ozone-induced damage on wheat yield and forest GPP in mainland China during 2010–2021. Ozone pollution caused a multiple-year average loss of 26.5 Mt for wheat yield and 552.6 TgC for forest GPP, accounting for 17% and 4% of the national total wheat yield and forest GPP without ozone impact, respectively. Due to the joint effects of ozone pollution, meteorological conditions and vegetation distribution, similarities and differences can be found in spatiotemporal distribution of wheat yield and forest GPP losses. Ozone-induced wheat loss commonly occurred in the East region and forest GPP losses in the South. Relatively heavy dual damages on both crop and forest are presented in some provinces of the two regions, and March–June is the period when dual damages occurred. The national ozone-induced wheat yield loss and forest GPP loss increased significantly at a rate of 1.8 Mt/yr and 13.9 TgC/yr during 2010–2021, respectively. The growth of ozone-induced damages was mainly driven by the elevated MDA8 ozone concentration in most regions. In East region, ozone pollution not only exerted a threat to vegetation, but also caused serious health burden. Enhanced efforts of ozone pollution alleviation in the polluted and developed regions in China are crucial for reducing ecological and health risks in the country.

Credit authors statement

Yutong Wang: Conceptualization, Methodology, Investigation, Formal analysis, Data curation, Visualization, Software, Writing – original draft preparation. **Youchao Wang**: Methodology, Investigation, Formal analysis, Data curation, Visualization, Software. **Zhaozhong Feng**: Resources, Writing – review & editing. **Xiangyang Yuan**: Writing – review & editing. **Yu Zhao**: Conceptualization, Resources, Writing – review & editing.

Declaration of competing interest

The authors declare that they have no known competing financial interests or personal relationships that could have appeared to influence the work reported in this paper.

Data availability

Data will be made available on request.

Acknowledgment

This project is supported by the National Natural Science Foundation of China (42177080, 41922052 and 42130714), Jiangsu Key Program of Science and Technology Demonstration for Social Development (BE2022838), and the Fundamental Research Funds for the Central Universities (0211/14380201).

Appendix A. Supplementary data

Supplementary data to this article can be found online at https://doi.org/10.1016/j.envpol.2023.121726.

References

Broberg, M.C., Feng, Z., Xin, Y., Håkan, P., 2015. Ozone effects on wheat grain quality - a summary. Environ. Pollut. 197, 203–213.
Dai, W., Jin, H., Zhang, Y., Liu, T., Zhou, Z., 2019. Detecting temporal changes in the temperature sensitivity of spring phenology with global warming: application of machine learning in phenological model. Agric. For. Meteorol. 279, 107702.
FAO, 2022. World food situation. http://www.fao.org/worldfoodsituation/csdb/en/.
Feng, Z., Kobayashi, K., Ainsworth, E.A., 2008. Impact of elevated ozone concentration on growth, physiology, and yield of wheat (Triticum aestivum L.): a meta-analysis. Global Change Biol. 14, 2696–2708.
Feng, Z., Pang, J., Kobayashi, K., Zhu, J., Ort, D.R., 2011. Differential responses in two varieties of winter wheat to elevated ozone concentration under fully open-air field conditions. Global Change Biol. 17, 580–591.
Feng, Z., Xu, Y., Kobayashi, K., Dai, L., Zhang, T., Agathokleous, E., Calatayud, V., Paoletti, E., Mukherjee, A., Agrawal, M., Rokjin, J., Yujin, J., Yue, X., 2022. Ozone pollution threatens the production of major staple crops in East Asia. Nature Food 3, 47–56.
Feng, Z., De Marco, A., Anav, A., Gualtieri, M., Sicard, P., Tian, H., Fornasier, F., Tao, F., Guo, A., Paoletti, E., 2019a. Economic losses due to ozone impacts on human health, forest productivity and crop yield across China. Environ. Int. 131, 104966.
Feng, Z., Kobayashi, K., Li, P., Xu, Y., Tang, H., Guo, A., Paoletti, E., Calatayud, V., 2019b. Impacts of current ozone pollution on wheat yield in China as estimated with observed ozone, meteorology and day of flowering. Atmos. Environ. 217, 116945.
Gong, C., Yue, X., Liao, H., Ma, Y., 2021. A humidity-based exposure index representing ozone damage effects on vegetation. Environ. Res. Lett. 16, 044030.
Huang, X., Shao, T., Zhao, J., Cao, J., Lv, X., 2020. Influencing factors of ozone concentration in Xi'an based on Generalized additive models. Environ. Sci. J. Integr. Environ. Res. 41, 1535–1542.
Li, K.D.J.J., Shen, L., Lu, X., Isabelle, D.S., Liao, H., 2020. Increases in surface ozone pollution in China from 2013 to 2019: anthropogenic and meteorological influences. Atmos. Chem. Phys. 20, 11423–11433.
Mills, G., Sharps, K., Simpson, D., Pleijel, H., Broberg, M., Uddling, J., Jaramillo, F., Davies, W.J., Dentener, F., Van den Berg, M., Agrawal, M., Agrawal, S.B., Ainsworth, E.A., Buker, P., Emberson, L., Feng, Z., Harmens, H., Hayes, F., Kobayashi, K., Paoletti, E., Van Dingenen, R., 2018. Ozone pollution will compromise efforts to increase global wheat production. Global Change Biol. 24, 3560–3574.
Monfreda, C., Ramankutty, N., Foley, J.A., 2008. Farming the planet: 2. Geographic distribution of crop areas, yields, physiological types, and net primary production in the year 2000. Global Biogeochem. Cycles 22, GB1022.
Mulder, C.P.H., Iles, D.T., Rockwell, R.F., 2017. Increased variance in temperature and lag effects alter phenological responses to rapid warming in a subarctic plant community. Global Change Biol. 23, 801–814.
Ren, X., Shang, B., Feng, Z., Calatayud, V., 2020. Yield and economic losses of winter wheat and rice due to ozone in the Yangtze River Delta during 2014-2019. Sci. Total Environ. 745, 140847.
Shi, X., Zheng, Y., Lei, Y., Xue, W., Yan, G., Liu, X., Cai, B., Tong, D., Wang, J., 2021. Air quality benefits of achieving carbon neutrality in China. Sci. Total Environ. 795, 148784.
Tai, A., Martin, M., 2017. Impacts of ozone air pollution and temperature extremes on crop yields: spatial variability, adaptation and implications for future food security. Atmos. Environ. 169, 11–21.
UNECE, 2017. Mapping Critical Levels for Vegetation. International Cooperative Programme on Effects of Air Pollution on Natural Vegetation and Crops (Bangor, UK).
Wang, H., Ge, Q., This, R., Dai, Y., Dai, J., 2015. Parameterization of temperature sensitivity of spring phenology and its application in explaining diverse phenological responses to temperature change. Sci. Rep. 5, 8833.
Xiao, Q., Geng, G., Xue, T., Liu, S., Cai, C., He, K., Zhang, Q., 2022. Tracking $PM_{2.5}$ and O_3 pollution and the related health burden in China 2013-2020. Environ. Sci. Technol. 56, 6922–6932.
Yue, X., Nadine, U., Kandice, H., Xia, X., Liao, H., Zhu, T., Xiao, J., Feng, Z., Li, J., 2017. Ozone and haze pollution weakens net primary productivity in China. Atmos. Chem. Phys. 17, 6073–6089.
Zhao, H., Zheng, Y., Wu, X., 2018. Assessment of yield and economic losses for wheat and rice due to ground-level O_3 exposure in the Yangtze River Delta, China. Atmos. Environ. 191, 241–248.
Zhang, K., Song, C., Zhang, Y., Zhang, Q., 2017. Natural disasters and economic development drive forest dynamics and transition in China. For. Pol. Econ. 76, 56–64.